Chapter 12

CROSSED-FIELD DEVICES

In the microwave devices we have described in previous chapters, the dc magnetic field has been used merely as a means of confining the electron beam to a given diameter. The beam focusing using the dc magnetic field and the rf interaction process have been considered as two independent problems. In crossed-field devices, on the other hand, the dc magnetic field plays a direct role in the rf interaction process. We shall find that amplifier gain, oscillator starting conditions, and power output are all functions of the dc magnetic field in crossed-field devices.

All crossed-field devices have one property in common. In the rf interaction space, there exists both a dc magnetic field and a dc electric field, perpendicular to each other. As an introduction to these devices, let us study the motion of a single electron in such a field configuration.

Figure 1.2-2 in Chapter 1 shows a rectangular coordinate system in a region of crossed electric and magnetic fields. The electric field intensity E is directed in the negative y direction, and the magnetic flux density B is directed in the negative z direction. We wish to study the motion of an electron which leaves the origin at time $t = 0$ with an initial velocity given by the three components u_{ox}, u_{oy}, and zero. Since there is no force in the z direction, the motion of the electron is constrained to the x-y plane.

The electron motion is given by the solution of Equations (1.2-10). The solutions for the instantaneous velocity and position are

$$u_x = \frac{dx}{dt} = \frac{E}{B} - \left(\frac{E}{B} - u_{ox}\right)\cos \omega_c t + u_{oy} \sin \omega_c t \tag{12-1}$$

$$u_y = \frac{dy}{dt} = \left(\frac{E}{B} - u_{ox}\right)\sin \omega_c t + u_{oy} \cos \omega_c t \tag{12-2}$$

and

$$x = \frac{E}{B}t - \frac{1}{\omega_c}\left(\frac{E}{B} - u_{ox}\right)\sin \omega_c t + \frac{u_{oy}}{\omega_c}(1 - \cos \omega_c t) \tag{12-3}$$

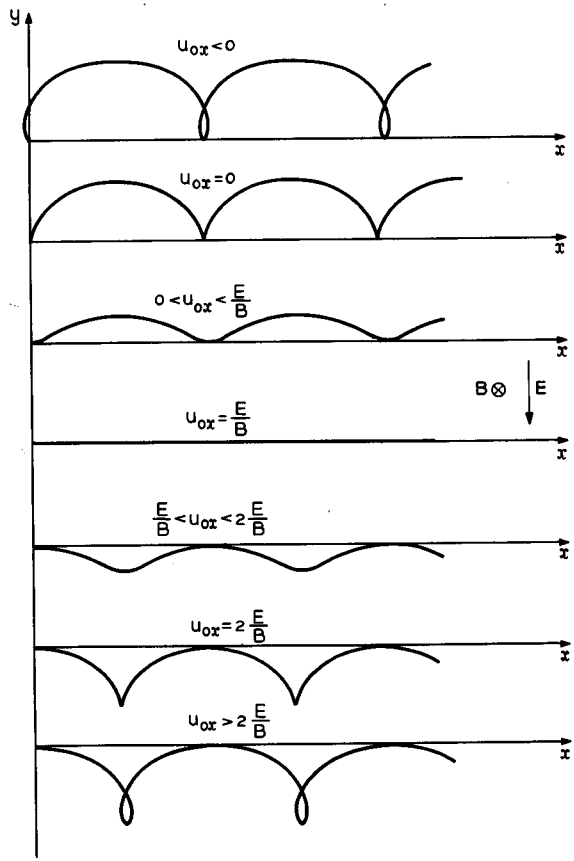

FIG. 12-1 Electron motion in a region of uniform, crossed dc electric and magnetic fields. Trajectories are shown for electrons with a zero y component of velocity at $x = 0$ and with various values for the x component.

$$y = \frac{1}{\omega_c}\left(\frac{E}{B} - u_{ox}\right)(1 - \cos \omega_c t) + \frac{u_{oy}}{\omega_c} \sin \omega_c t \tag{12-4}$$

where

$$\omega_c = \frac{eB}{m}$$

is the cyclotron frequency in radians per second. The electron trajectories determined by these equations are shown in Figure 12-1 for $u_{oy} = 0$ and various values of u_{ox}.

Solutions for non-zero values of u_{oy} are similar; the trajectories are obtained from Figure 12-1 by translating the x-y coordinate system so that the origin falls at other points on the trajectories. In this case, a value of u_{ox} given in the figure is interpreted as the x component of velocity along the trajectory for which the y component is zero.

The solutions exhibit several interesting properties.

1. The motion is cycloidal except for the case $u_{ox} = E/B$, $u_{oy} = 0$, for which the electron moves in a straight line. In this particular case, the force due to the electric field is exactly balanced by the force due to the magnetic field.
2. The frequency of the cycloidal motion is given by the cyclotron frequency and is thus a function only of the magnetic field and the charge-to-mass ratio for an electron.
3. The average drift velocity in the x direction is given by E/B, completely independent of the initial velocities u_{ox} and u_{oy}.

Item number 3 is of particular interest. An approximate picture of the electron motion in a region of crossed electric and magnetic fields can be obtained by neglecting the cyclic motion of the electron and considering only the average motion. This average motion is perpendicular to both E and B and has a magnitude E/B. It is a function only of the fields at the location of the electron and does not depend on the electron's past history. Thus, the electron tends to follow an equipotential line of the electric field.

The basic elements of a crossed-field device are shown in Figure 12-2.[1]

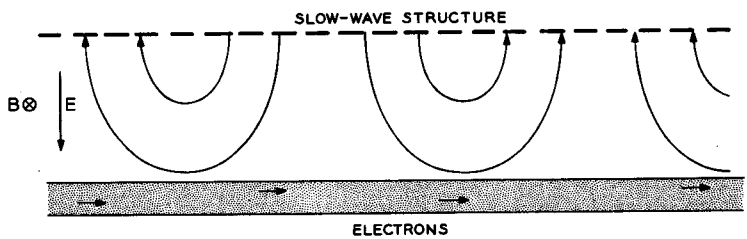

FIG. 12-2 Basic elements of a crossed-field device. Rf electric field lines due to a traveling-wave on the slow-wave structure are pictured at a particular instant of time.

Electrons are traveling parallel to a slow-wave structure. There is a dc electric field E directed as shown away from the slow-wave circuit and a dc magnetic field B directed into the page. The dc motion of the electrons is

[1]This linear model is useful for analysis. Practical crossed-field devices are usually constructed in a cylindrical configuration, as we shall see later.

assumed to be as in Figure 12-1 for $u_{oz} = E/B$. The slow-wave structure is assumed to be propagating a wave in the direction of the electron flow with a phase velocity equal to E/B. Thus, some form of synchronous interaction is evidently possible between the electrons and the electromagnetic wave.

We can view the interaction from a frame of reference traveling to the right with a velocity E/B. In this reference frame both the electromagnetic wave and the electrons appear motionless until we include the effect of the rf electric field on the electron motion.

The trajectories which result when we include the effect of the rf electric field are shown in Figure 12-3. These trajectories are derived using the

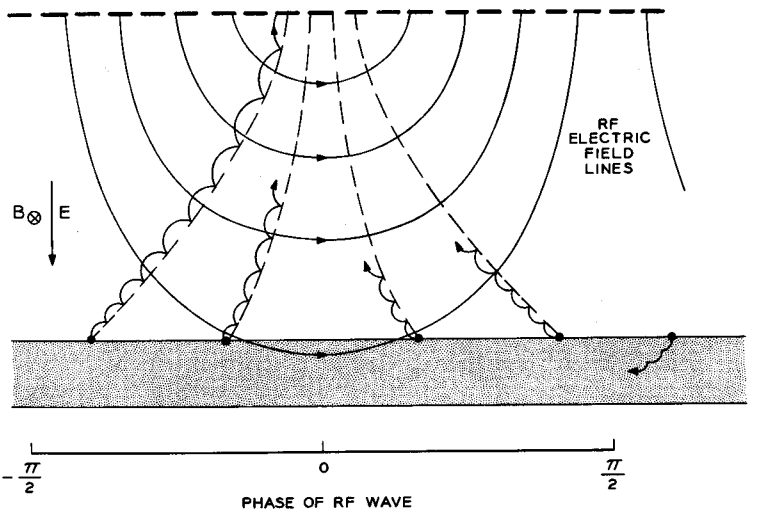

FIG. 12-3 Electron trajectories in a reference frame synchronous with the rf traveling wave. Space-charge forces are neglected. The average drift motion of the electrons is seen to be along lines orthogonal to the electric field lines.

following reasoning. In the reference frame the rf electric field appears stationary. Thus, we may consider the electron motion to be determined by static fields, the electric field having spatial dependence but no time dependence. If we assume that the electric field's spatial dependence is slow and continuous, we may use the solutions previously derived for a constant field, which are illustrated in Figure 12-1. Thus, the motion has a cycloidal appearance with a net drift of the electron along a path orthogonal to the electric field lines. The cycloidal amplitude and period vary monotonically corresponding to the monotonically increasing strength of the

electric field as the slow-wave structure is approached. For simplicity, space-charge forces are neglected.

The average kinetic energy of the electron at any position is determined from the average drift velocity, given by

$$u_{\text{avg}} = \frac{E_T}{B} \tag{12-5}$$

where E_T is equal to the sum of the dc electric field and the rf electric field at the position under consideration. Since the rf field is strongest at the slow-wave structure, and decays monotonically away from it, the electron continuously gains average kinetic energy as it drifts toward the slow-wave structure. On the other hand, the electron loses dc potential energy of an amount given by the product: $eE \times$ (displacement of the electron in the direction of the slow-wave circuit). *This dc potential energy loss is greater than the increase in kinetic energy of the electron; the balance of the energy is delivered to the rf field by the mechanism of induced currents.* That is, each electron continuously induces a current in the slow-wave circuit; the power delivered by each electron to the circuit is proportional to the dot product of the total electron velocity and the rf electric field.

Electrons in phases given by $\pi/2 < |\theta| < \frac{3}{2}\pi$ (see Figure 12-3) move away from the slow-wave structure rather than toward it. These electrons extract a net amount of energy from the rf field. However, since the rf electric field is much weaker for these electrons than for the group which moves toward the circuit, there is still a large net transfer of energy to the rf field. In a magnetron oscillator the electrons which move away from the slow-wave circuit return to the cathode and serve the useful purpose of heating it so that less heater power is required. They also liberate secondary electrons which constitute a large percentage of the total emission.

Approximate trajectories which neglect the cycloidal motion are indicated by dotted lines in Figure 12-3. These trajectories are constructed by drawing lines orthogonal to the E-field lines. The average velocity in the reference frame at any point is $1/B$ times the rf electric field at that point.

One important characteristic of crossed-field devices should be noted at this time. As the electrons interact with the rf field, they remain in synchronism with it until they are finally collected on the slow-wave structure. Crossed-field devices are said to convert potential energy into rf energy, since the electron's kinetic energy in the direction of propagation of the rf wave is essentially unchanged. This is in contrast to the klystron and the traveling-wave tube, wherein rf energy is derived from the longitudinal kinetic energy of the electrons. The fact that the electrons remain locked to (or phase focused by) the rf wave, even at extremely large signal levels, leads to very high electronic efficiencies in crossed-field devices. Efficiencies of 70 per cent and higher have been obtained.

In the following sections we shall examine three classes of crossed-field devices, the magnetron, the crossed-field amplifier, and the M-carcinotron. Because of the inherent complexity of the two-dimensional electron motion in crossed fields, we shall restrict ourselves to somewhat idealized models of the physical phenomena. This idealized approach is also necessitated by the fact that there is not complete agreement among individuals working in the field as to the correct approach to some of the basic theoretical problems.

12.1 Magnetrons

A schematic illustration of the functional parts of a magnetron oscillator is shown in Figure 12.1-1. A cylindrical cathode is surrounded by an

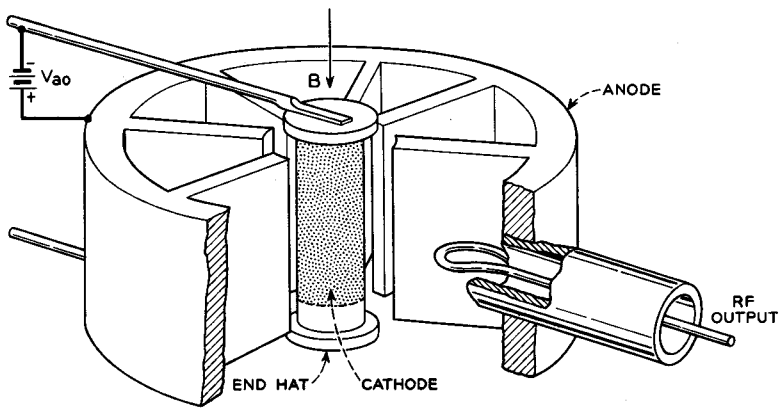

FIG. 12.1-1 A magnetron oscillator.

anode consisting of a re-entrant slow-wave structure. A uniform magnetic field, parallel to the cylindrical axis, fills the region between cathode and anode.

Electrons emitted from the cathode would flow radially to the anode were it not for the magnetic field, which causes the electron trajectories to be bent. In the crossed-field geometry of Figure 1.2-2, the maximum distance an electron can penetrate toward the anode is obtained from Equation (12-4). We see that this distance is inversely proportional to the strength of the magnetic field. Neglecting the effect of the rf field, a sufficiently large magnetic field causes most of the electrons to turn back toward the cathode before reaching the anode. This results in a dense, turbulent sheath of electrons rotating about the cathode.

The slow-wave structure propagates an electromagnetic wave around its circumference with the average angular speed of the electrons. This pro-

duces an interaction of the type described in connection with Figure 12-3. Electrons flow to the anode in "spokes" which are synchronous with the rf wave. See Figure 12.1-2. The re-entrant nature of the slow-wave structure provides a built-in feedback mechanism which permits oscillations to

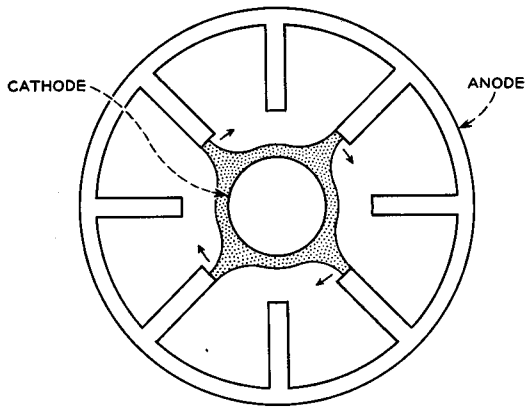

FIG. 12.1-2 Approximate shape of the space-charge configuration in the interelectrode space of a magnetron. This configuration rotates, giving the appearance of the spokes and hub of a wheel.

occur. One period of the slow-wave structure bounded by two vanes is referred to as a resonator. One of the resonators of the slow-wave structure is coupled inductively to a loop formed from the center conductor of a coaxial cable. The coaxial cable in turn delivers the rf output signal to the load.

The end hats on the cathode structure are at cathode potential but nonemitting. They serve to prevent the electrons from spreading axially out of the interaction space.

The slow-wave structure in the magnetron of Figure 12.1-1 is essentially a folded version of the structure of Figure 8.7-4. The Brillouin diagram for this structure was presented in Figure 8.7-8. The portion of this diagram currently of interest is replotted in Figure 12.1-3, where φ is the phase shift per period.

Since the circuit is closed on itself, or "re-entrant," oscillations are possible at frequencies for which the total phase shift around the circuit is an integral multiple of 2π radians. Thus, if N is the total number of periods of the slow-wave structure, oscillations can occur at the frequencies corresponding to

$$\varphi = \frac{2\pi n}{N} \tag{12.1-1}$$

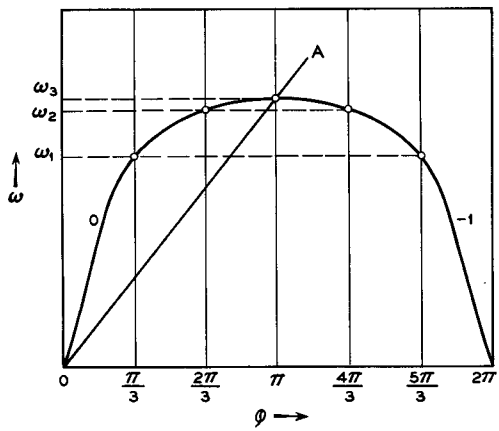

FIG. 12.1-3 Brillouin diagram for the slow-wave structure of a magnetron. Points at which oscillations are possible are indicated for a re-entrant structure 6 periods long.

where n is an arbitrary integer. These values of phase shift and the corresponding frequencies are indicated by points in Figure 12.1-3 for $N = 6$.

In order for oscillations to be produced at these points, two conditions must be fulfilled. First, the anode voltage V_{ao} must be adjusted so that the average rotational velocity corresponds to the phase velocity of the slow-wave structure. Second, the beam-coupling impedance must be sufficiently large. The operating points shown in Figure 12.1-3 are termed modes of oscillation, with the mode identified by stating the phase shift per cavity.

Although oscillations are theoretically possible in any of the modes given by Equation (12.1-1), the magnetron is always designed for operation in the π mode because this allows the strongest possible interaction. Thus, in Figure 12.1-3, the magnetron is designed to oscillate at a radian frequency ω_3.

Magnetrons are usually operated with the voltage V_{ao} pulsed on and off, so as to produce short pulses of rf signal. As the voltage is increased toward the value corresponding to the π mode, it must necessarily pass through the points of synchronism with other modes ($4\pi/3$ and $5\pi/3$ modes in Figure 12.1-3). Since spurious oscillations in these modes are undesirable, it is necessary to design the slow-wave structure carefully to avoid them. Either the beam-coupling impedance must be too low for oscillations, or else the losses associated with these modes must be large enough to prevent oscillation buildup in the time available.

The magnetron as described thus far oscillates at only one frequency, the frequency corresponding to the π mode of the slow-wave structure.

Such fixed-frequency magnetrons have very limited application; some form of tunability is highly desirable. Tuning of the magnetron is accomplished by means of a mechanical perturbation of the slow-wave structure. This causes a change in the Brillouin diagram with a consequent change in the π mode frequency ω_3. One way of tuning the structure of Figure 12.1-1 is to insert a uniform array of metal pins into the inductive regions of the resonators, one pin in each resonator. This causes a reduction in the inductance of each resonator so that the frequency ω_3 is increased, the increase being proportional to the depth of penetration. Practical schemes for electronic tuning of magnetrons have not been developed at the time of writing.

Oscillation in the π mode is unique in that the electrons are actually synchronous with two space harmonics simultaneously. These space harmonics are: First, the fundamental space harmonic corresponding to power flow in the direction of the electron flow, and second, the -1 space harmonic corresponding to power flow in the opposite direction. Since the circuit is cut off at this frequency, the net power flow in either direction is zero. Thus the two power flows described above are equal and opposite. Space-harmonic analysis reveals that the two space harmonics described above are excited to equal amplitude at π phase shift per period, for equal power flow in the two directions. Thus, the summation of the two synchronous waves and their space harmonics corresponds to a standing wave as in any microwave cavity at resonance. Interaction phenomena is thus conveniently described in terms of the cavity Q's — the unloaded Q, external Q, and loaded Q — as defined in Chapter 9 for the klystron.

In the case of the π mode, the synchronous electromagnetic wave described in connection with Figures 12-2 and 12-3 is interpreted as the superposition of the two synchronous space harmonics described above.

(*a*) *The Hull Cutoff Condition*

We are ready to consider some of the quantitative aspects of magnetron interaction. First, we shall consider a model of the electron motion which includes space-charge forces but excludes all rf fields. This is known as the static magnetron problem. Instead of the re-entrant cylindrical structure used in most magnetron oscillators, we shall consider the linear magnetron structure shown in Figure 12.1-4. This model exhibits all of the essential characteristics of the cylindrical version, without the attendant mathematical complexity. A uniform dc magnetic field B is directed into the page. The solution we wish to demonstrate is one in which the electrons all move in straight lines from left to right with velocity E/B. We have already noted that this type of motion is possible for an individual elec-

tron, so that the problem that remains is that of finding the potential and charge distribution in the interelectrode space when many electrons are present. Because of the planar geometry, we must assume that when the electrons reach the right-hand end of the model of Figure 12.1-4, they disappear and reappear at the left-hand end.

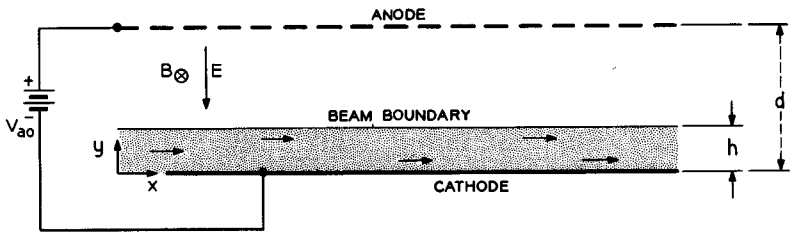

FIG. 12.1-4 Linear model of a magnetron. Rf fields may be precluded by replacing the slow-wave structure by a uniform conducting plane.

The dc voltage V_{ao} applied between the slow-wave structure (anode) and the cathode causes a dc electric field $E(y)$ directed away from the anode.

Using the coordinate axes shown in Figure 12.1-4, the electron motion is assumed to be such that all electrons flow to the right with a velocity given by

$$u_x = \frac{E(y)}{B} = \frac{1}{B}\frac{dV}{dy}$$

$$u_y = u_z = 0 \tag{12.1-2}$$

where V is the electrostatic potential, a function of y. The dc electric field $E(y)$ is a function of the y coordinate within the beam because of the space charge. The beam lies within a region extending a distance h from the cathode, where h is known as the hub thickness.[2]

Next, we solve for the electrostatic potential within the beam. If the electrons originated at the cathode, energy conservation would indicate that

$$\tfrac{1}{2}mu_x^2 = eV \tag{12.1-3}$$

Eliminating u_x between the last two equations gives us

$$\left(\frac{dV}{dy}\right)^2 = 2\frac{e}{m}B^2V \tag{12.1-4}$$

[2]This stream of electrons is referred to as the hub, since in the cylindrical magnetron it has the appearance of the hub of a wheel.

This differential equation may be rearranged as

$$\frac{1}{\sqrt{2\frac{e}{m}B}}\frac{dV}{\sqrt{V}} = dy \tag{12.1-5}$$

in which form it may be integrated directly, with the solution

$$V = \frac{eB^2}{2m}y^2 \tag{12.1-6}$$

for the potential within the beam. The constant of integration has been eliminated assuming $V = 0$ at $y = 0$.

The potential and electric field at the hub surface are obtained from Equation (12.1-6) as

$$V(h) = \frac{e}{2m}B^2h^2 \tag{12.1-7}$$

and

$$E_y = -\frac{dV}{dy} = -\frac{e}{m}B^2h \tag{12.1-8}$$

From Section 8.3, we know that the electric field must be continuous across the beam boundary. Therefore, Equation (12.1-8) gives the electric field in the region $h \leq y \leq d$. The potential at the anode is thus obtained from Equation (1.1-6) as

$$\begin{aligned} V_{ao} &= -\int_0^d E_y dy \\ &= -\int_0^h E_y\, dy - \int_h^d E_y dy \\ &= V(h) + \frac{e}{m}B^2h(d - h) \\ &= \frac{e}{m}B^2h(d - h/2) \end{aligned} \tag{12.1-9}$$

where use has been made of Equation (12.1-7). This equation allows one to calculate the hub thickness for various values of magnetic field and anode voltage.

From Poisson's Equation, Equation (1.4-9), one may calculate the charge density within the hub from Equation (12.1-6) as the constant value

$$\rho = -\frac{e\varepsilon_o}{m}B^2 \tag{12.1-10}$$

From Equation (12.1-9) we may calculate the threshold anode voltage for which the anode draws current. This occurs when the hub thickness h is exactly equal to the spacing d. This voltage is known as the Hull cutoff voltage, given by

$$V_{ao} = \frac{1}{2}\frac{e}{m}B^2d^2 \tag{12.1-11}$$

This relationship is plotted in Figure 12.1-5. For operating points below the parabola of this figure, the anode theoretically will not draw current.

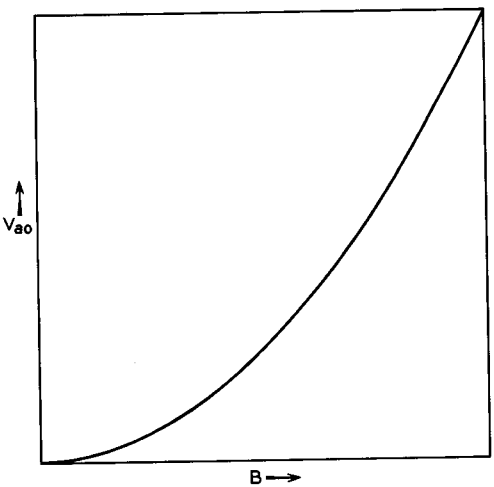

FIG. 12.1-5 Hull cutoff voltage for a magnetron. For voltages below the parabola, the anode theoretically will draw no current.

It is interesting to note that Equation (12.1-11) is a consequence of the law of conservation of energy. Thus the same result is obtained for any other assumed set of electron trajectories or distribution of charge density, provided that they are independent of the x coordinate. This can be shown very easily as follows. An electron leaving the cathode with zero velocity of emission arrives at the anode with a kinetic energy given by

$$\tfrac{1}{2}m[u_x^2 + u_y^2]_{y=d} = eV_{ao} \tag{12.1-12}$$

From a single integration of the first of Equations (1.2-10), we have

$$u_x = \frac{e}{m}By \tag{12.1-13}$$

where use has been made of the initial condition $u_x = 0$ at $y = 0$. Com-

bining the last two equations, we obtain

$$V_{ao} = \frac{1}{2}\frac{e}{m}B^2d^2 + \frac{1}{2}\frac{m}{e}[u_y^2]_{y=d} \qquad (12.1\text{-}14)$$

Cutoff occurs for $u_y = 0$ at the anode, obtaining Equation (12.1-11).

A typical experimental curve[3] of anode current as a function of anode voltage is shown in Figure 12.1-6 for a cylindrical magnetron with a constant value of magnetic field. Also shown is the corresponding curve for zero magnetic field. The latter curve exhibits the three-halves power dependence of current on voltage as given by Equation (4.1-10) up to the point where the emission becomes temperature limited. The experimental curve with a non-zero magnetic field is characterized by three segments as indicated in the figure.

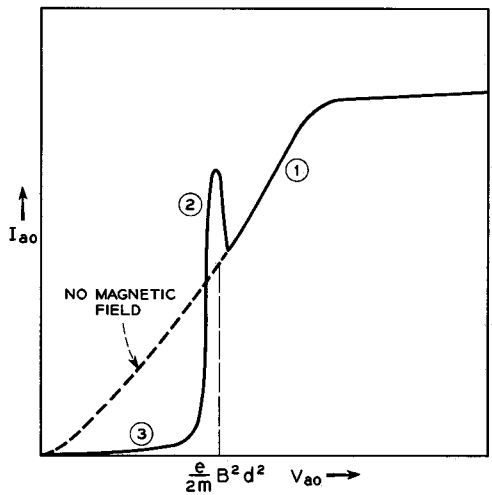

FIG. 12.1-6 Experimental variation of anode current with anode voltage for a constant magnetic field in a magnetron without an rf circuit.

Segment 1 occurs for very large values of anode voltage. Here the electric field force is so strong compared with the magnetic field force that the electrons travel nearly radially to the anode; the situation is essentially the same as for zero magnetic field.

Segment 2 occurs for voltages approximately equal to the Hull cutoff value. In this region the current increases rapidly as the voltage is raised, reaches a maximum, and then abruptly falls to the value corresponding to

[3]Reference 12.1.

Segment 1. Segment 3 shows a small, non-zero anode current for voltages below the Hull cutoff value.

The existence of anode current for voltages below the Hull cutoff value is in direct violation of the Hull cutoff theory, indicating the inadequacy of this theory. A number of hypotheses have been proposed to explain this behavior.[4] Certainly, the idealized electron flow assumed in Figure 12.1-4 is not readily attained. Perturbations of this flow give rise to space-charge fields which tend to push certain of the electrons to the anode and others back to the cathode.[5] This instability results in anode current, emission of secondary electrons from the cathode and additional heating of the cathode due to the electron back bombardment, and the generation of excess rf noise. The overall picture is complicated by the spread of electron emission velocities and electron-electron collisions in the hub. These effects are most pronounced for voltages near the Hull cutoff value. For this condition the amount of rotating space charge is the greatest, and hence the conditions for space-charge instabilities are most favorable.

In spite of the experimental contradictions to the electron flow model of Figure 12.1-4, we shall assume in subsequent discussion that the model provides a first approximation to the unperturbed electron flow in the magnetron. The presence of the electromagnetic field due to a slow-wave structure will act as a strong perturbation on this model, an effect which will be considered in the next section. We may consider the perturbations discussed in the previous paragraph to be negligible in comparison.

(*b*) *The Hartree Condition*

The Hull cutoff condition (Figure 12.1-5) determines the anode voltage necessary to obtain non-zero anode current as a function of the magnetic field in the absence of electromagnetic fields. In this section we shall consider a second condition which must be imposed on B and V_{ao}. If interaction is to take place between the electrons and the rf wave propagating along the slow-wave circuit, the electron velocity parallel to the circuit must be approximately equal to the phase velocity of the wave. This leads to a relationship between B and V_{ao} known as the Hartree condition.

The Hartree condition is determined as follows. Electron flow is assumed to exist as in Figure 12.1-4. The hub thickness h is of the order of one fourth the cathode-anode spacing d. Now if a weak electromagnetic wave is present, electron flow to the anode is possible, as in Figure 12-3, provided that the electrons are in synchronism with the wave. Since the electrons

[4]Reference 12a, Vol. 1, pp. 179–326, 359–366.

[5]This perturbed flow produces space-charge forces in the x direction so that Equation (12.1–13) is no longer valid.

at the hub surface ($y = h$) have the greatest velocity, the threshold anode voltage for oscillation is determined by the condition of synchronism of these electrons with the rf wave.

The velocity of electrons at the hub surface is obtained from Equations (12.1-2) and (12.1-8) as

$$u_x(h) = \frac{e}{m}Bh \tag{12.1-15}$$

For synchronism, this is equal to the phase velocity of the slow-wave structure,

$$\frac{\omega}{\beta} = \frac{e}{m}Bh \tag{12.1-16}$$

where β is the circuit propagation constant at the desired operating point. For the π mode, β is given by

$$\beta L = \pi \tag{12.1-17}$$

where L is the period of the circuit. At the onset of oscillations we may neglect the presence of space charge exterior to the hub. Thus, Equation (12.1-9) determines the anode voltage as a function of the hub thickness. The hub thickness may be eliminated between Equations (12.1-9) and (12.1-16), obtaining

$$V_{ao} = \frac{\omega Bd}{\beta} - \frac{m}{2e}\frac{\omega^2}{\beta^2} \tag{12.1-18}$$

This is the Hartree condition.

The Hartree voltage is plotted as a function of the magnetic field in Figure 12.1-7, together with the Hull cutoff curve. The usual operating region of a magnetron is shown in the figure. Below this region, neither oscillation nor appreciable anode current is obtained. Above this region, anode current independent of the rf properties of the circuit would be obtained. Typically, the operating point is quite close to the Hartree line in order to avoid spurious oscillations in higher voltage modes. Thus, the hub thickness is a small fraction of the cathode-anode spacing.

Within the region of operation, raising the anode voltage causes increased anode current and rf power output. The velocity of the electrons at the surface of the hub is obtained from the relations of Section 12.1(a) as

$$u_x(h) = \frac{eBd}{m}\left[1 - \sqrt{1 - \frac{2mV_{ao}}{eB^2d^2}}\right] \tag{12.1-19}$$

As the anode voltage is raised above the Hartree value, this velocity increases above the synchronous value. Nonetheless, the forces due to the rf field tend to pull these electrons back into synchronism with the wave.

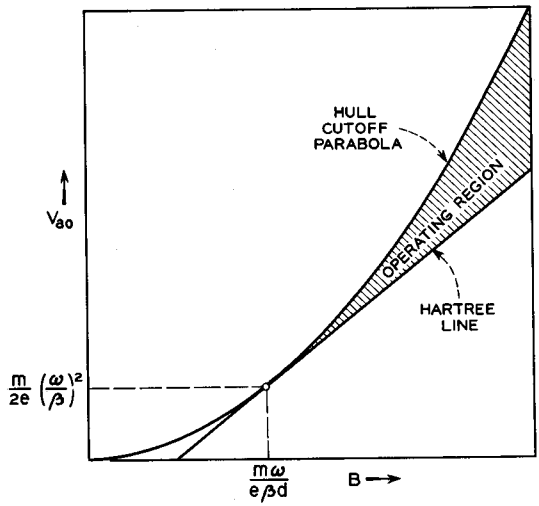

FIG. 12.1-7 Region of operation of a magnetron, between the Hartree line and the Hull cutoff parabola.

This behavior is shown in the computed trajectories of Figure 12.1-8.[6] The trajectories correspond to electrons leaving the hub surface with average velocities in the x direction given by Equation (12.1-19) for three different anode voltages. Space-charge forces are neglected. Figure 12.1-8(a) shows the trajectories at the Hartree voltage; electrons leave the hub in synchronism with the wave and remain in synchronism with it up to the anode. Figure 12.1-8(b) shows the trajectories for a somewhat higher anode voltage, representing typical magnetron operation. Although the electrons start out faster than the wave, they are phase focused back by the rf field forces so that the spoke is nearly centered about zero phase. Zero phase corresponds to the maximum rf electric field and consequently to the position of strongest interaction. Figure 12.1-8(c) shows the trajectories at still a higher value of anode voltage. Once again we see the focusing action of the rf field. The noncycloidal trajectories of Figure 12.1-8 are approximate in that the initial acceleration at the hub surface is arbitrarily set to zero. The cycloidal trajectories in Figure 12.1-8(c) illustrate the trajectories resulting without this approximation.

As the level of oscillation is increased, the average center of the spoke tends to advance in phase with respect to the wave. This has the effect of an inductive loading of the circuit, and the frequency of oscillation

[6] J. Feinstein, Reference 12a, Vol. 1, pp. 554–579.

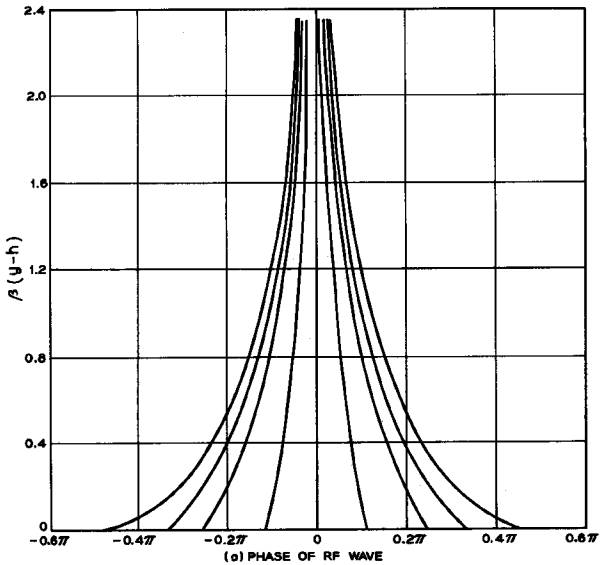

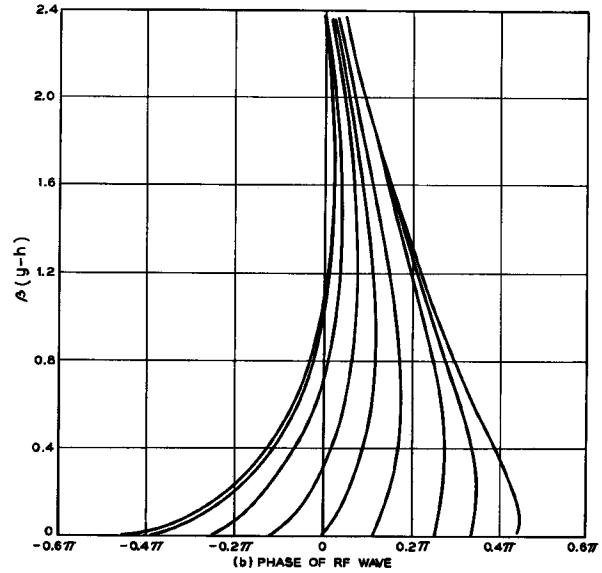

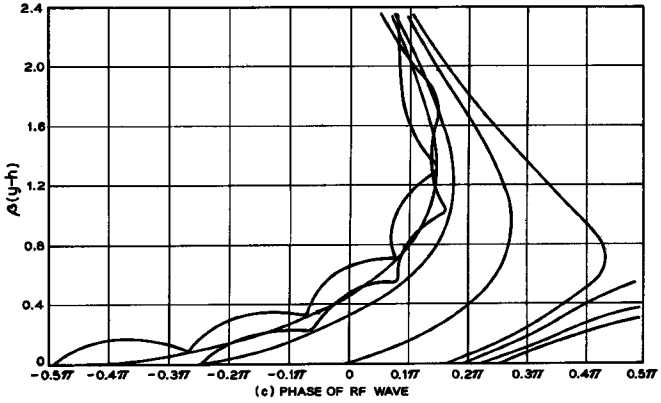

FIG. 12.1-8 Computed electron trajectories in a reference frame synchronous with the rf wave on the circuit, neglecting space-charge forces. Zero phase corresponds to a maximally retarding field, as in Figure 12-3. (a) Trajectories for operation at the Hartree voltage; the oscillation level is low. (b) Trajectories at a typical rf level of operation. (c) Trajectories at a very high rf level of operation (Reference 12a). (Courtesy of Academic Press, Inc.)

consequently increases slightly. This effect is known as frequency pushing. Its magnitude is too small to provide a practical means for electronic tuning

Further calculations of the type shown in Figure 12.1-8 indicate that there is a minimum or threshold value for the rf electric field in order to obtain a stable current spoke for each value of anode voltage greater than the Hartree value. Below this threshold the electrons do not form a spoke but instead are returned to the hub.

(c) *Power Output and Efficiency*

The efficiency of the magnetron is the ratio of the rf power output to the product of anode voltage and anode current. It may be expressed in turn as the product of the electronic efficiency η_e and the circuit efficiency η_c. The electronic efficiency expresses the percentage of the dc or pulsed input power which is converted into rf power on the slow-wave structure. The circuit efficiency, on the other hand, determines the percentage of this rf power which is delivered to the load exterior to the tube.

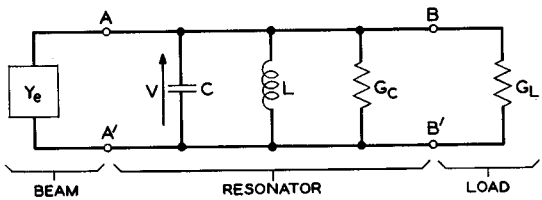

FIG. 12.1-9 Equivalent circuit for one resonator of a magnetron. The symbols are defined in the text.

The circuit efficiency may be evaluated in terms of the equivalent circuit presented in Figure 12.1-9. Each resonator of the slow-wave structure is taken to comprise a separate resonant circuit, with equivalent circuit parameters C, L, and G_c. Thus for vane resonators, as shown in Figure 12.1-1, C is the capacitance at the vane tips, including fringing capacitance. From a knowledge of C and the resonant frequency, the inductance L can be determined. The resonant frequency of each individual resonator is taken as the π mode frequency of the whole anode structure. A conductance G_c is chosen so as to give the correct value of rf loss on the anode circuit per resonator. The unloaded Q of the magnetron is thus

$$Q_u = \frac{\omega_o C}{G_c} \tag{12.1-20}$$

where ω_o is the radian resonant frequency.

The rf voltage across the vane tips (terminals AA') is given by the phasor V. G_L is the equivalent load conductance per resonator chosen in such a

manner as to give the power delivered to the load per resonator. The anode circuit and load are connected at terminals BB' by various components such as coupling loops, transformers, lengths of transmission line, etc., which usually introduce reactive effects and loss by their presence. For simplicity, we neglect these effects. The external Q is defined by

$$Q_e = \frac{\omega_o C}{G_L} \tag{12.1-21}$$

The loaded Q of the circuit is given by

$$Q_l = \frac{\omega_o C}{G_c + G_L} \tag{12.1-22}$$

and the Q's are related by Equation (9.1-33). It is to be noted that the values of the Q's are the same when defined for the anode structure as a whole, since they represent ratios of energy stored to energy dissipated.

The circuit efficiency is given by

$$\eta_c = \frac{G_L}{G_L + G_c} \tag{12.1-23}$$

which may be written in terms of the Q's as

$$\eta_c = \frac{Q_l}{Q_e} = \frac{1}{1 + \frac{Q_e}{Q_u}} \tag{12.1-24}$$

Maximum circuit efficiency is obtained when the magnetron is loaded very heavily by the load, that is, for $G_L \gg G_c$. However, heavy loading makes the tube operation quite sensitive to the load, which is undesirable in some cases. Because of the reactive effects associated with the load and output coupling circuit, load changes can cause shifts in the frequency of oscillation. Therefore, the ratio of Q_l/Q_e chosen is often a compromise between the conflicting requirements for high circuit efficiency and frequency stability.

The electronic admittance due to the electrons is represented by Y_e in Figure 12.1-9. This admittance has a negative conductance representing the power generated and a small inductive susceptance whose variation with oscillation level produces frequency pushing. This latter effect was discussed in the previous section.

The electronic efficiency may be obtained from the following formula:

$$\eta_e = \frac{P_{\text{gen}}}{V_{ao} I_{ao}} = \frac{V_{ao} I_{ao} - P_{\text{lost}}}{V_{ao} I_{ao}} \tag{12.1-25}$$

where P_{gen} is the rf power induced into the anode circuit by the electrons, V_{ao} is the anode voltage, I_{ao} is the anode current, and P_{lost} is the power

lost in the tube other than the rf losses in the slow-wave structure and output circuit.

P_{lost} consists of two main parts. The largest loss is the anode dissipation, given by the kinetic energy of the electrons striking the anode. A much smaller loss is due to the back bombardment of the cathode; electrons in unfavorable phases gain energy from the rf field and return to the cathode with an excess of kinetic energy. The back bombardment is usually 3 to 10 per cent of the input power.[7]

The kinetic energy of the electrons reaching the anode may be estimated in the following manner. From trajectory plots as in Figure 12.1-8 we conclude that it is approximately correct to assume that all the electrons arrive at the anode in zero phase of the rf wave. Thus, if E_{max} is the maximum value of the x component of the synchronous space harmonic of the rf electric field, the average y component of the velocity of the electrons on striking the anode is approximately

$$u_y(d) = \frac{E_{max}}{B} \tag{12.1-26}$$

using Equation (12-5). The average value of the x component of velocity is approximately given by the synchronous value,

$$u_x(d) = \frac{\omega}{\beta} \tag{12.1-27}$$

The rf power generated by the electrons is given by

$$\begin{aligned} P_{gen} &= I_{ao}V_{ao} - P_{lost} \\ &= I_{ao}V_{ao} - I_{ao}\frac{m}{2e}[u_x^2(d) + u_y^2(d)] \\ &= I_{ao}V_{ao} - I_{ao}\frac{m}{2e}\left[\frac{\omega^2}{\beta^2} + \frac{E_{max}^2}{B^2}\right] \end{aligned} \tag{12.1-28}$$

where use has been made of Equations (12.1-26) and (12.1-27). The power loss associated with cathode back-bombardment is neglected for the time being.

From the equivalent circuit of Figure 12.1-9 we have the following expression for the power generated by the electrons,

$$P_{gen} = \frac{1}{2}N \mid V \mid^2 \frac{\omega C}{Q_l} \tag{12.1-29}$$

where N is the total number of resonators comprising the anode structure, and V is the rf voltage appearing across the resonator gap. The amplitudes

[7] A. M. Clogston, Reference 12b, p. 525.

of the space harmonics may be determined by space-harmonic analysis as in the preceding chapters. The amplitude of the x component of the electric field at the circuit is given by

$$E_{\max} = \frac{M_1 |V|}{L} \tag{12.1-30}$$

where M_1 is the gap factor for the π mode, computed from Equation (10.2-20), and L is the center-to-center spacing of the vane tips. The power generated may thus be written as

$$P_{\text{gen}} = \frac{NL^2\omega C}{2M_1^2 Q_l} E_{\max}^2 \tag{12.1-31}$$

$E_{\max}^2$ may be eliminated between Equations (12.1-28) and (12.1-31) and the result solved for P_{gen}. One then obtains the following expression for the electronic efficiency:

$$\eta_e' = \frac{P_{\text{gen}}}{I_{ao} V_{ao}} = \frac{1 - \dfrac{m\omega^2}{2eV_{ao}\beta^2}}{1 + \dfrac{I_{ao}}{B^2}\dfrac{mM_1^2 Q_l}{eNL^2\omega C}} \tag{12.1-32}$$

where the prime indicates that the cathode back-bombardment power loss has been neglected. Using this formula, one may evaluate the influence of the various magnetron parameters on the electronic efficiency. Since ω/β is approximately E/B, both numerator and denominator approach unity as the magnetic field is increased. Thus, magnetrons are designed to operate at as high a magnetic field as can be conveniently obtained in order to achieve high electronic efficiency.

Decreasing Q_l would increase the electronic efficiency but decrease the circuit efficiency. Also, a low value of Q_l makes it difficult to start the oscillations in the desired mode. The value of Q_l is thus a compromise between the values for best overall efficiency and ease of starting oscillations.

In the following section we shall describe a typical magnetron, the Western Electric 7208B. The parameters of this magnetron which appear in Equation (12.1-32) are:

$f = 16.5$ Gc	$Q_u = 4000$
$V_{ao} = 17.5$ kv	$C = 0.15$ pf
$I_{ao} = 16.8$ amps	$N = 32$
$B = 0.74$ webers/meter^2	$L = 0.94$ mm
$Q_l = 1025$	$M_1^2 = 0.762$

Using Equation (12.1-32) one calculates

$$\eta_e' = 64\%$$

If we assume that the cathode back-bombardment power loss is 6 per cent of the input power, we obtain the net electronic efficiency,

$$\eta_e = 58\%$$

From Equations (9.1-33) and (12.1-24), the circuit efficiency is calculated as

$$\eta_c = 74\%$$

resulting in an overall efficiency of

$$\eta = \eta_c \eta_e = 43\%$$

an excellent value of efficiency for an oscillator at such a high frequency. This corresponds to an output power of 126 kw.

(*d*) *Description of the Western Electric 7208B Magnetron*

The Western Electric 7208B magnetron is shown in Figure 12.1-10.[8] This tube is operated with the anode voltage pulsed on and off so that short

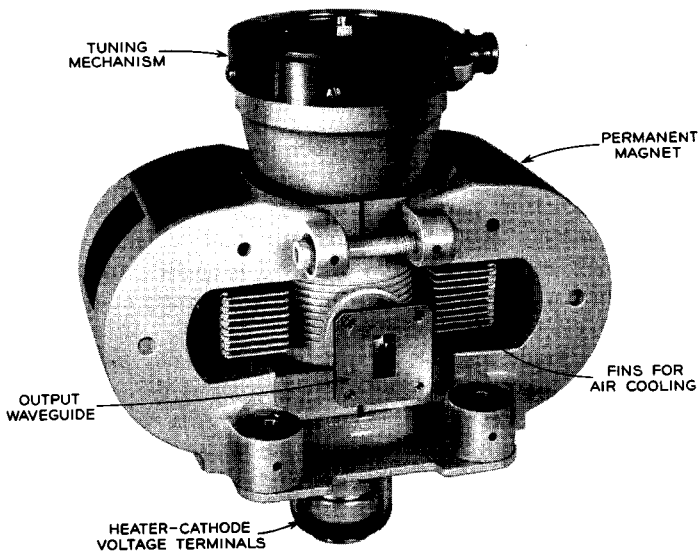

FIG. 12.1-10 Western Electric 7208B magnetron, complete with permanent magnet. The complete unit weighs 14 pounds and is 20 cm high.

pulses of rf power are produced. The rf output frequency is mechanically tunable over the range 15,500 to 17,500 Mc. Typical operating characteristics are listed in Table 12.1-1.

---

[8]Reference 12.2.

TABLE 12.1-1. W.E. 7208B TYPICAL OPERATING CHARACTERISTICS

Frequency, Mc	15,500 to 17,500
Peak power output, kw	125
Peak anode voltage, kv	17.5
Peak anode current, amps	19
Current pulse duration, microsec	3
Duty cycle	0.001
Magnetic field, webers/m²	0.74
Pulling figure (VSWR = 1.5:1), Mc	6

The pulling figure is defined as the total variation in frequency when the phase of a mismatched load is varied through all values. A voltage-

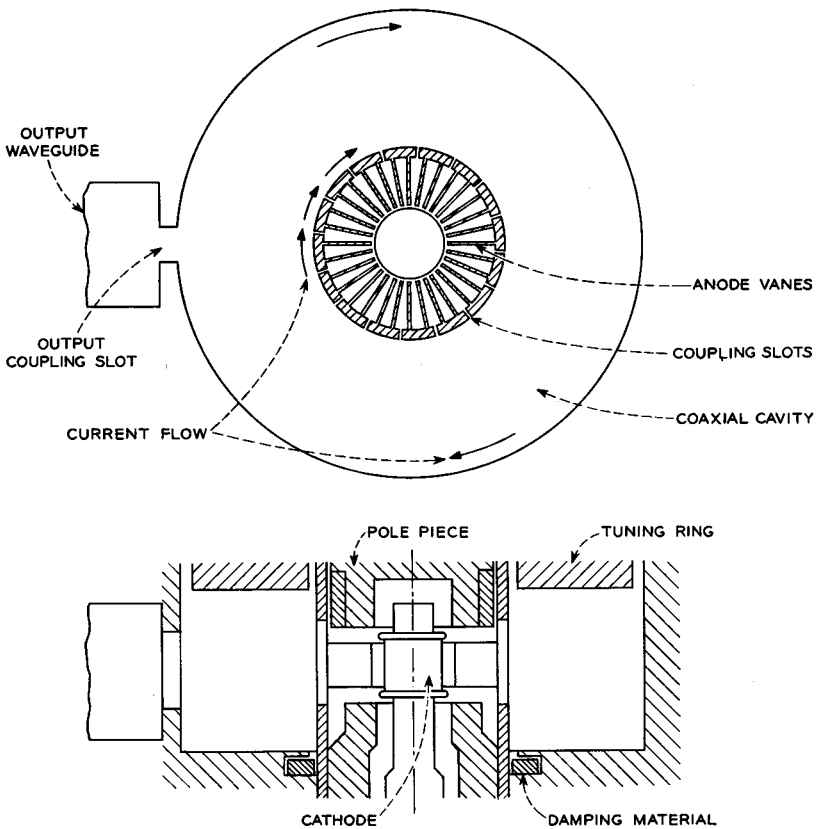

FIG. 12.1-11 Functional drawing of the Western Electric 7208B.

standing-wave ratio (VSWR) of 1.5 to 1 is equivalent to a mismatch such that 4 per cent of the output power is reflected back into the tube.

The maximum duty cycle of the 7208B is 0.001, where

$$\text{duty cycle} = \frac{\text{average power output}}{\text{peak power output}} \tag{12.1-33}$$

Another useful formula for the duty cycle is

$$\text{duty cycle} = (\text{pulse length}) \times (\text{pulse repetition frequency}) \tag{12.1-34}$$

Most magnetrons are designed to be pulse operated. This form of operation is particularly useful in radar systems. Since the magnetron anode is grounded, pulsed operation is achieved by applying negative, rectangular-shaped voltage pulses to the cathode.

The 7208B magnetron is of a type known as a coaxial magnetron because of the particular anode slow-wave structure used. A functional drawing of the tube is shown in Figure 12.1-11. The anode consists of a cylinder with vanes extending radially toward the cathode. This anode cylinder also forms the center conductor of a coaxial resonator. Every other resonator in the vane array is coupled to the coaxial resonator by means of a slot in the common wall.

Since the vanes are approximately a quarter wavelength long in the radial direction, the impedance seen at the slot looking toward the vane tips is very small. Thus, circumferential current may flow unimpeded on the

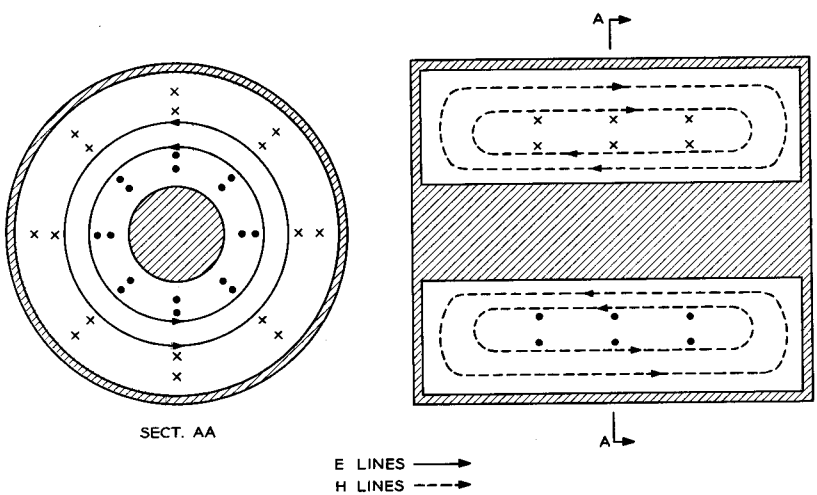

FIG. 12.1-12 Field patterns of the TE_{011} mode in a coaxial resonator.

outer surface of the anode in much the same way as if it were unslotted. We may therefore consider the coaxial cavity to have the same field patterns as for the case of a solid cylindrical center conductor,

The desired mode of operation for the coaxial resonator is the TE_{011} mode, whose field patterns are shown in Figure 12.1-12. Since the wall currents are perpendicular everywhere to the magnetic field lines, we see that the field patterns for the TE_{011} mode correspond to circumferential current flow on all the wall surfaces. There is no current flow in either the radial or axial direction. Since there is no current flow across from the coaxial cylinders to the end plates, a gap may exist between these surfaces without disturbing the field patterns. This permits the incorporation of a tuning ring, as shown in Figure 12.1-11, so that the length of the coaxial resonator may be varied. Since the resonant frequency of the cavity increases as the cavity length is decreased, this provides a means for tuning the cavity.

The currents entering the vane array through the coupling slots have the same phase in each of the slotted resonators. Hence, the fields in each of the slotted resonators are in phase. Currents are induced in the unslotted resonators by virtue of the mutual coupling between adjacent resonators. These induced currents are 180 degrees out of phase with the currents in the slotted resonators. Hence the field components in adjacent resonators are 180 degrees out of phase. This produces the desired π-mode field configuration.

Because of the tight coupling of the vane array to the high-Q coaxial cavity, the π-mode frequency is essentially that of the coaxial cavity alone. The unloaded Q of the 7208B is 4000 at midband. Rf power output is coupled from the coaxial cavity to a waveguide by means of a coupling slot as shown in Figure 12.1-11. This results in a midband loaded Q of approximately 1025.

Pole pieces are built right into the tube so as to concentrate the magnetic flux in the interaction space. The horseshoe-shaped permanent magnets provide a magnetic flux density of 0.74 webers/meter^2 in this region. The tube, complete with magnets, weighs 14 pounds and is 20 cm high.

The damping material indicated in Figure 12.1-11 damps out resonant modes of the cavity with current flow patterns across the junctions of cylindrical surfaces and end walls. As indicated above, the TE_{011} mode does not fall into this category, and consequently it is not damped by this lossy material. If this damping material were not present, troublesome oscillations could occur in modes other than the desired one.

A magnetron performance chart is an instructive manner of presenting the important operating characteristics. Such a chart is shown in Figure 12.1-13 for the 7208B. Primarily, the chart is a plot of anode voltage vs.

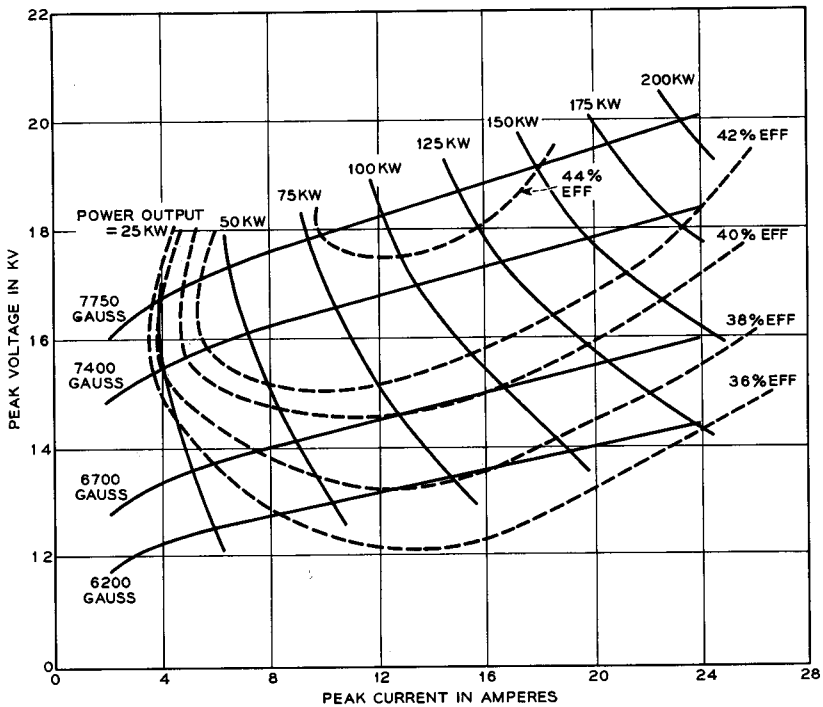

FIG. 12.1-13 Performance chart of the Western Electric 7208B at a frequency of 16.5 Gc. The usual operating magnetic field is 7400 gauss, furnished by the permanent magnets.

anode current at a fixed frequency, with magnetic field as a parameter. Variation of the magnetic field is achieved by operating the tube in an electromagnet. Contours of constant power output and constant efficiency are also included. As the voltage is raised, the anode current and power output increase rapidly. The power output increases almost in direct proportion to the power input. The upper limit on power output is usually reached when arcing commences in the tube due to the high electric fields.

As the anode voltage is increased, the efficiency first increases and then decreases, for constant magnetic field. Equation (12.1-32) demonstrates this behavior. For small anode current, the efficiency goes up as V_{ao} increases. Physically, this corresponds to a decreasing percentage of the total energy associated with the synchronous velocity of the electrons. As the anode current I_{ao} becomes appreciable, the efficiency begins to fall off. This corresponds to the increasing percentage of the electron kinetic energy associated with velocity directed toward the anode.

Magnetrons provide a compact, high-efficiency source of rf power with an operating voltage which is relatively low in comparison with other tubes of similar power output. Because of cathode back-bombardment, anode erosion due to electron bombardment, and other factors, magnetrons tend to have shorter life than other microwave tubes. Magnetrons have a lower signal-to-noise ratio than other microwave tubes; however, for most power tube applications, this is not important. The noisiness is primarily due to the excitation of other modes of the resonant system. Unlike the reflex klystron and the backward-wave oscillator, where the frequency is voltage tunable, the frequency of the magnetron is determined primarily by the resonant frequency of the anode structure; hence, stability of the output frequency in the magnetron is attained without precise regulation of the supply voltage. On the other hand, the requirement of mechanical tuning in the magnetron prohibits the use of the magnetron in applications where extremely rapid tuning is desired.

12.2 Crossed-Field Amplifiers

The crossed-field amplifier[9] is very similar to the magnetron oscillator, both in internal construction and external appearance. The only important difference is that the anode slow-wave structure of the amplifier does not close on itself. Instead, the two ends of the circuit are both connected to separate external transmission lines, one for the input and one for the output rf signal.

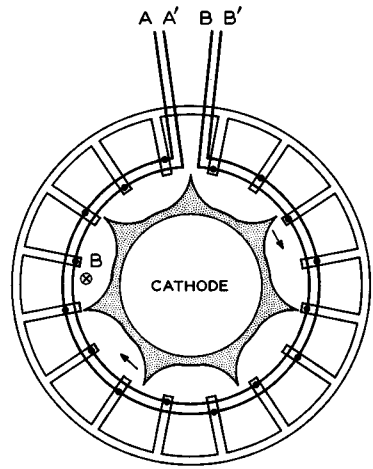

FIG. 12.2-1 Schematic drawing of a crossed-field amplifier.

A schematic drawing of the crossed-field amplifier is shown in Figure 12.2-1. An applied voltage and dc magnetic field are provided as in the magnetron oscillator. Spokes of current are formed by the rf electric fields. These spokes rotate in a clockwise direction around the cathode. For forward-wave interaction, rf power enters at terminals BB', flows around the circuit in a

[9]This discussion is limited to crossed-field amplifiers having a continuous cathode with a re-entrant beam. Crossed-field amplifiers have also been constructed where the electron beam is injected into the interaction region and then collected (as in Figure 12.3-1); however, the latter device has not been as widely used as the device considered here.

clockwise direction, and exits at terminals AA'. The current spokes travel in synchronism with the circuit wave, inducing currents in phase with those of the circuit wave, thus causing it to grow. This interaction mechanism is like that of the magnetron oscillator, except that the circuit wave grows with distance whereas it is of constant amplitude in the oscillator.

Alternatively, backward-wave interaction is obtained when the rf power is introduced at terminals AA' and removed at terminals BB'. This is actually the mode of operation for the particular circuit shown in Figure 12.2-1.[10] This circuit consists of a two-wire line with connections made alternately to the vanes, as shown. It is a fundamental backward-wave structure.[11]

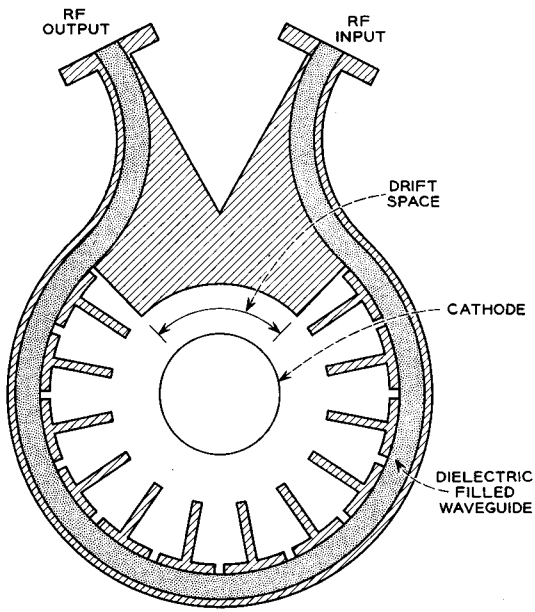

FIG. 12.2-2 A crossed-field amplifier with a drift region between the input and output ends of the rf circuit.

Although the circuit is non-re-entrant, the beam is re-entrant. As a result, the crossed-field amplifier could oscillate if the loop gain were high enough. This limits the gain to about 10 or 15 db in high-power amplifiers

[10]Reference 12.3.

[11]Slow-wave structures are characterized as either fundamental forward or fundamental backward wave structures, depending upon whether the space harmonic of greatest amplitude is a forward or a backward wave.

with a circuit completely around the circumference, as in Figure 12.2-1. The spoke moves from the output end of the circuit to the input end, phased so as to produce positive feedback and high efficiency. This phasing condition limits the bandwidth to the order of 10 to 15 per cent.

Some crossed-field amplifiers are built with the circuit encompassing only a fraction of the total circumference as illustrated in Figure 12.2-2.[12] This results in a significant drift space for the electron beam between the two ends of the circuit. In this drift space, the electron spokes are considerably dispersed by the space-charge forces, thus reducing the feedback mechanism of the electron stream. As a result, gains of the order of 15 to 20 db are possible. Since loop phasing of the electron stream is not critical, this type of crossed-field amplifier is capable of wider bandwidths. On the other hand, the reduction of positive feedback results in a lower electronic efficiency.

The anode slow-wave structure presented in Figure 12.2-2 consists of a waveguide periodically coupled by slots to each resonator of the anode vane array. The waveguide is filled with dielectric so that the phase velocity is slowed down to the synchronous velocity of interaction. Interaction is with the fundamental forward-wave space harmonic.

Crossed-field amplifiers are designed with the rf electric field at the input strong enough to form a complete current spoke of the type shown in Figure 12.1-8(a). Thus, fully formed spokes are present at all positions along the circuit. Under this condition both theoretical and experimental evidence indicates that the power induced into the circuit by each spoke and the dc current per spoke are nearly constant, independent of both the spoke location and the rf electric field at that point.

Each current spoke induces two circuit waves, one traveling toward the input, the other toward the output. However, only the waves traveling toward the output add in phase. The waves traveling toward the input tend to cancel each other so that the net power out of the input port is very small. Since each spoke induces equal power into the circuit, the circuit wave grows with a power increasing linearly with distance from input to output.

Since the circuit wave growth is linear, increasing gain from 10 db to 20 db corresponds to increasing circuit length by a factor of ten. In contrast, exponential wave growth achieves this gain increase with a doubling of the circuit length. This is another reason why crossed-field amplifiers typically exhibit low values of gain.

The total power generated in a given crossed-field amplifier is independent of the rf power input, so long as the input power exceeds the thresh-

[12] J. Feinstein and R. J. Collier, Reference 12a, Vol. 2, pp. 211–222.

old value for spoke stability at the input. The power generated can be increased only by increasing the anode voltage and current. This behavior is illustrated in Figure 12.2-3. Neglecting circuit attenuation, the

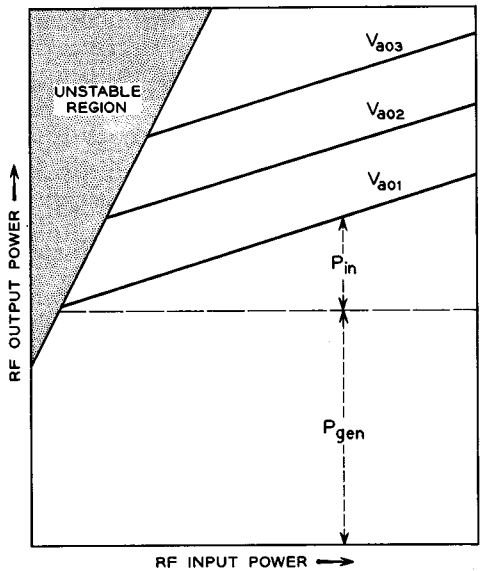

FIG. 12.2-3 Rf output power as a function of rf input power, with anode voltage as a parameter. The rf power generated P_{gen} and the rf input power P_{in} are indicated for the lowest anode voltage. V_{ao1}, V_{ao2}, and V_{ao3} indicate successively increasing anode voltages.

output power is given by the sum of the input power and the power generated (which is constant for constant anode voltage). Thus, the amplifier gain is a function of the power input. That is,

$$\text{gain} = \frac{P_{in} + P_{gen}}{P_{in}} = 1 + \frac{P_{gen}}{P_{in}} \tag{12.2-1}$$

Therefore, the device is not a linear amplifier but rather is termed a saturated amplifier.

If the rf drive is insufficient to form a stable current spoke at the input, no gain is produced and no power is generated at the desired frequency. Instead spurious oscillations are produced which may be attributed to the re-entrant nature of the beam and the inherent instability of electrons in crossed fields. These spurious oscillations become "locked out" when the tube is amplifying normally at the input frequency.

Since high efficiency is one of the principal attributes of the crossed-field amplifier, let us derive an expression for this quantity in terms of the various tube parameters.

The efficiency may be defined as the product of the electronic efficiency η_e and the circuit efficiency η_c. The electronic efficiency is defined as in Equation (12.1-25). The overall efficiency is defined as

$$\eta = \frac{P_{\text{out}} - P_{\text{in}}}{V_{ao}I_{ao}} \tag{12.2-2}$$

where P_{out} and P_{in} are the rf power ouput and input for the tube, respectively. It is necessary to include the latter quantity in the definition of efficiency since it is usually an appreciable percentage of the output power. For example, if the gain of the tube is 6 db, then P_{in} would be 25 per cent of P_{out}. This sizable contribution must be subtracted from the output power in order to obtain an accurate evaluation of the efficiency of conversion of dc to rf energy. The circuit efficiency is thus obtained from Equations (12.1-25) and (12.2-2) as

$$\eta_c = \frac{\eta}{\eta_e} = \frac{P_{\text{out}} - P_{\text{in}}}{P_{\text{gen}}} \tag{12.2-3}$$

Since the power generated per unit length is constant, the output power is given by

$$\begin{aligned} P_{\text{out}} &= P_{\text{in}}\epsilon^{-2\alpha l} + \int_0^l \frac{P_{\text{gen}}}{l}\epsilon^{-2\alpha(l-x)}dx \\ &= P_{\text{in}}\epsilon^{-2\alpha l} + \frac{P_{\text{gen}}}{2\alpha l}(1 - \epsilon^{-2\alpha l}) \end{aligned} \tag{12.2-4}$$

where α is the attenuation constant of the circuit, and l is the circuit length. Introducing this expression into Equation (12.2-3) results in the following expression for the circuit efficiency:

$$\eta_c = \left[\frac{1}{2\alpha l} - \frac{P_{\text{in}}}{P_{\text{gen}}}\right](1 - \epsilon^{-2\alpha l}) \tag{12.2-5}$$

The term $P_{\text{in}}/P_{\text{gen}}$ becomes negligible for high gain devices.

Next we calculate an expression for the electronic efficiency. Starting with Equation (12.1-25) an analysis is made similar to that for the magnetron oscillator. It is assumed that the input signal is sufficiently strong for spoke stability and that the rf power grows linearly with distance along the circuit. We further assume that the dc current per spoke is a constant, independent of the rf level at any point. The loss due to back-bombardment is not considered at this time. We assume that the circuit runs com-

pletely around the circumference, as in Figure 12.2-1. We shall show later how the result may be modified to apply to circuits that do not.

The energy lost by the electrons on striking the anode is equal to their kinetic energy and consists of two parts, corresponding to the two velocity components given by Equations (12.1-26) and (12.1-27). The velocity given by Equation (12.1-26) increases with position along the circuit since the rf field is increasing. The rf field is related to the power flow at any point by the definition of the beam-coupling impedance at the circuit,

$$K = \frac{E_{\max}^2}{2\beta^2 P} \tag{12.2-6}$$

The value of impedance is taken at a specific point, rather than being averaged across the beam as in Equation (10.1-19). The point at which it is taken is adjacent to the anode circuit, corresponding to a maximum value of the x component of the synchronous space harmonic, $E_{\max}$.

Using Equations (12.1-26) and (12.2-6), the power lost per spoke due to the motion toward the anode is given at any position by

$$P_s = I_{so}\frac{m}{e}\frac{\beta^2 K P}{B^2} \tag{12.2-7}$$

where I_{so} is the dc current per spoke, and P is the power flow on the circuit at the position considered. Since the power varies linearly with position, the average loss over the circuit length is

$$P_{s\,\text{avg}} = I_{so}\frac{m}{e}\frac{\beta^2 K}{2B^2}(P_{\text{in}} + P_{\text{out}}) \tag{12.2-8}$$

The total power loss for all the spokes is obtained using Equations (12.1-27), (12.2-1), and (12.2-8) as

$$P_{\text{lost}} = \frac{1}{2}I_{ao}\frac{m}{e}\left(\frac{\omega}{\beta}\right)^2 + I_{ao}\frac{m}{e}\frac{\beta^2 K}{2B^2}\left(\frac{\mathcal{G}+1}{\mathcal{G}-1}\right)P_{\text{gen}} \tag{12.2-9}$$

where $\mathcal{G}$ is the power gain.

The expression for the electronic efficiency is obtained by combining Equations (12.1-25) and (12.2-9) as

$$\eta_e' = \frac{1 - \dfrac{m\omega^2}{2eV_{ao}\beta^2}}{1 + \dfrac{I_{ao}}{B^2}\dfrac{m\beta^2 K}{2e}\left(\dfrac{\mathcal{G}+1}{\mathcal{G}-1}\right)} \tag{12.2-10}$$

where the prime indicates that loss due to back-bombardment of the cathode has not been included. Comparing this result with the corresponding result for the magnetron, Equation (12.1-32), we note a strong similar-

ity. Designing for high efficiency in both devices involves optimizing more or less the same parameters.

Equation (12.2-10) applies to a circuit which runs completely around the circumference of the tube. A rough estimate of the efficiency for a tube with a drift space can be obtained in the following manner. The total anode current is assumed to be independent of the length of the drift space. The power generated, on the other hand, must be only a fraction F of the power generated using a circuit covering the whole circumference, where F is the fraction of the circumference covered. Thus, the electronic efficiency is F times the value for a tube with no drift space.

Let us calculate the efficiency of a typical crossed-field amplifier with the following parameters:

$$\begin{aligned} f &= 9100 \text{ Mc} \\ V_{ao} &= 35.8 \text{ kv} \\ I_{ao} &= 18.5 \text{ amps} \\ B &= 0.40 \text{ weber/meter}^2 \\ \beta &= 1155 \text{ radians/meter} \\ K &= 120 \text{ ohms} \\ \mathcal{G} &= 10 \\ 2\alpha l &= 0.230 \text{ (1 db attenuation)} \\ P_{\text{in}} &= 42 \text{ kw} \end{aligned}$$

These parameters apply to an experimental tube assembled at Bell Telephone Laboratories. From Equation (12.2-10), we calculate the value

$$\eta_e' = 69\%$$

If we subtract 5 per cent for back-bombardment of the cathode, the net electronic efficiency becomes

$$\eta_e'' = 64\%$$

for a circuit completely around the circumference. In the particular experimental tube whose parameters are given above, the circuit covered only three fourths of the circumference ($F = \frac{3}{4}$). Therefore,

$$\eta_e = F\eta_e'' = 48\%$$

for this particular tube.

In order to calculate the circuit efficiency using Equation (12.2-5), we must first calculate P_{gen} from the value of electronic efficiency obtained above. We obtain

$$P_{\text{gen}} = \eta_e I_{ao} V_{ao} = 316 \text{ kw}$$

From Equation (12.2-5), the circuit efficiency is calculated as

$$\eta_c = 87\%$$

so that the overall efficiency is

$$\eta = \eta_c \eta_e = 42\%$$

A value of 43 per cent was measured on this experimental tube. This value would be improved considerably if the length of the drift space were reduced.

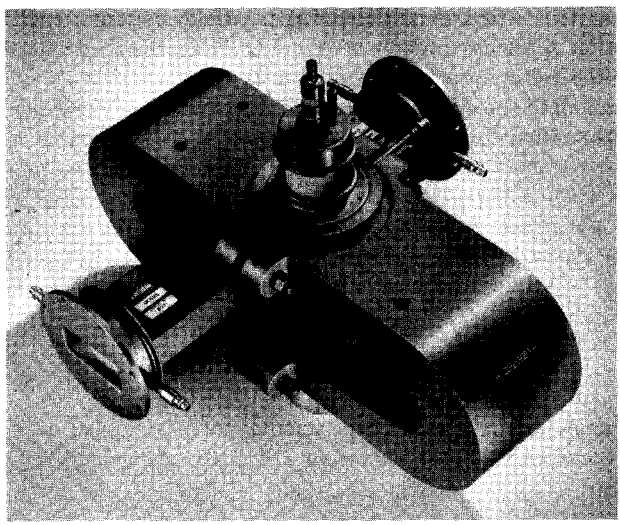

FIG. 12.2-4 Raytheon RK8129 *Amplitron*. The tube weighs 110 pounds with magnet, and it fits within a 51-cm cube. (Courtesy of Raytheon Company)

Next, we present a description of a particular crossed-field amplifier, the Raytheon RK8129 *Amplitron*,[13] pictured in Figure 12.2-4. Typical

TABLE 12.2-1. RK8129 *Amplitron* TYPICAL OPERATING CHARACTERISTICS

Frequency, Mc	2900 to 3100
Peak power output, Mw	3
Average power output, kw	15
Peak anode voltage, kv	50
Peak anode current, amps	66
Peak rf input power, kw (minimum)	550
Gain, db	8
Pulse duration, microsec	10
Efficiency, %	78

[13] *Amplitron* is a Raytheon trade name for a magnetron amplifier. The RK8129 is also designated the QK622.

operating characteristics of this tube are tabulated in Table 12.2-1.[14] The device is characterized by an extremely high efficiency, albeit the gain is only 8 db. Such a tube is useful as the final stage in a high-power transmitter, where over-all efficiency is the prime consideration.

High electronic efficiency is obtained through the use of an anode circuit of the type shown in Figure 12.2-1, with essentially a zero-length drift space. Since the circuit attenuation is less than 0.5 db, the circuit efficiency is also high.

Typical operating characteristics are shown as a function of frequency in Figure 12.2-5. The curves shown are for constant rf input signal, with the peak $V_{ao}I_{ao}$ product held approximately constant. The latter condition is automatically obtained when the anode voltage pulses are obtained from

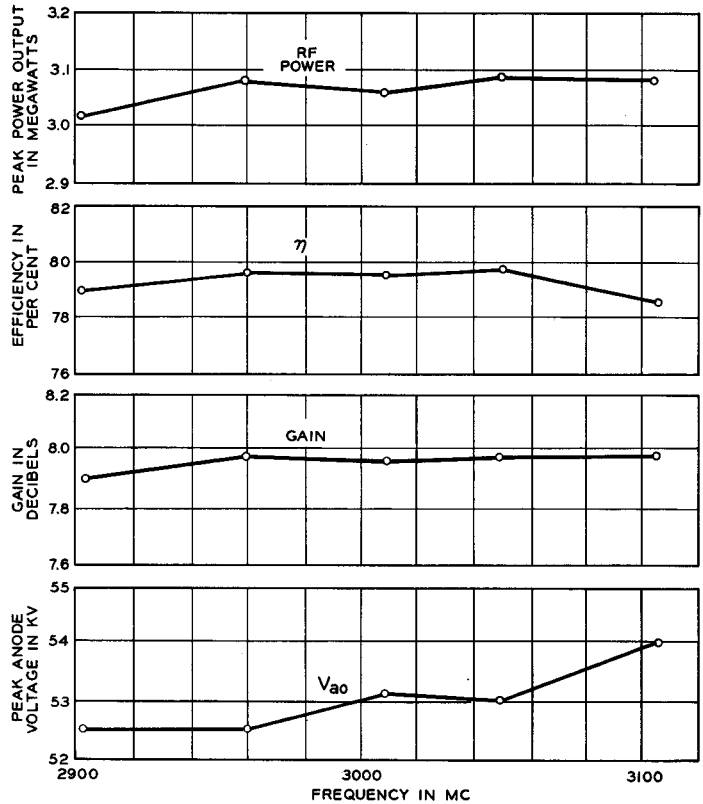

FIG. 12.2-5 RK8129 typical operating characteristics. The rf input power and peak anode current are held constant at 490 kw and 62 amps, respectively. (Courtesy of Raytheon Company)

[14]Reference 12.4.

a line-type modulator.[15] The power output and gain are seen to vary little over the frequency band.

Tubes of this type have been operated in parallel to obtain additional power.

Proper operation of crossed-field amplifiers prohibits the application of anode voltage unless an rf signal is being applied at the input. This prevents the generation of spurious rf output signals, which could possibly damage the tube. These spurious signals result from the basic instabilities of electrons in crossed fields.

Because of the phase locking phenomenon in crossed-field amplifiers, the phase pushing is very small. In the RK8129, the phase changes 0.5 degree per 1 per cent change in peak anode current.

Crossed-field amplifiers have a number of attributes. They provide a compact, high-efficiency amplifier with fractional bandwidths of the order of 10 per cent and relatively low-voltage operation. The efficiency is typically higher than that of the magnetron oscillator and substantially higher than that of the traveling-wave or klystron amplifier. When the tube is used as a power output tube in a radar installation, rf signals received by the antenna may be passed through the tube to the lower rf level input waveguide before they are separated from the common transmit-receive circuit. This is possible because there is no sever in the anode circuit. A simpler duplexer[16] can therefore be used. Another attribute is the low phase pushing. Cold cathode operation is possible, thus eliminating the necessity of a high-voltage-insulated heater supply.

On the other hand, the crossed-field amplifier has several disadvantages in comparison with klystron amplifiers and traveling-wave amplifiers. Since it is a saturated amplifier, it cannot successfully transmit amplitude modulated signals. The low gain requires the use of a high-power traveling-wave tube or klystron as a driver tube. The noise level is high, as is typical of all crossed-field tubes.[17] The fact that the electron beam must be dissipated on the anode slow-wave structure presents serious cooling problems at high power levels.

12.3 M-Carcinotron Oscillators

The M-carcinotron oscillator[18] is a backward-wave oscillator in which the

[15]An anode voltage source where the voltage pulse is obtained by discharging an artificial transmission line using a thyratron as a switch.

[16]A duplexer is a device which alternately connects the transmitter and receiver circuits to a radar antenna.

[17]Recent experiments have indicated that the noise is not inherently high in injected-beam crossed-field amplifiers (footnote 9); see Reference 12.6.

[18]Also known as an M-type backward-wave oscillator. To avoid ambiguity, the device of Chapter 11 is termed an O-type backward-wave oscillator.

interaction between the electrons and the slow-wave structure takes place in a region of crossed dc fields.

A linear version of an M-carcinotron is shown in Figure 12.3-1. A slow-wave structure is arranged parallel to an electrode known as the sole. With

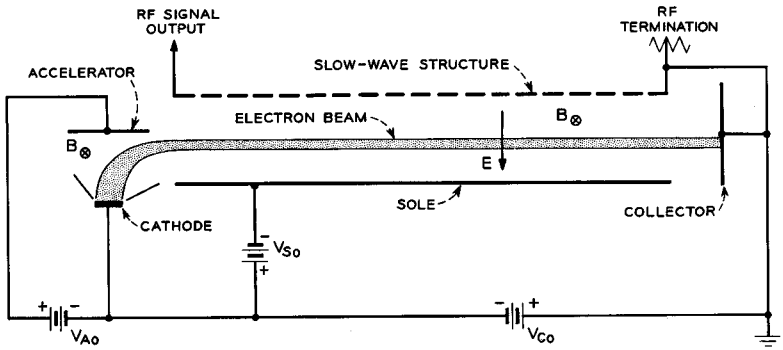

FIG. 12.3-1 Linear version of an M-carcinotron oscillator.

the slow-wave structure at ground potential, a voltage V_{So} is provided to make the sole negative. This produces a dc electric field as shown. A dc magnetic field is directed into the page. As indicated in the figure, this magnetic field is also present in the electron gun region.

The electron gun is different from the electron guns in Chapter 4, because of the action of the magnetic field. The electrons are drawn from the cathode toward the accelerator by the accelerator voltage V_{Ao}. However, the magnetic field causes the electron trajectories to be curved through a 90-degree angle as shown. At this point the electrons leave the gun region and enter the interaction region. If the voltages are chosen properly, the electrons enter the interaction region with a velocity E/B so that they travel parallel to the circuit,[19] until they are finally collected by the collector electrode. Since the cathode surface is rectangular, a rectangular sheet beam is formed.

The rf interaction is similar to that of the backward-wave oscillator. The electrons interact with a backward-wave space harmonic of the circuit, the energy on the circuit flowing opposite to the direction of the electron motion. This provides the feedback necessary for oscillation. The circuit is terminated at the collector end, and the rf signal is removed at the gun end.

---

[19]This neglects the rf perturbations of the electron motion which will be considered later.

The interaction with the backward-wave space harmonic may be discussed in connection with Figure 12.3-2. A line is drawn from the origin with a slope given by E/B, the drift velocity of the electrons. The intersection of this line with the backward-wave space harmonic determines the frequency at which the space-harmonic phase velocity equals the electron drift velocity, the synchronism condition. Thus oscillations are produced at a radian frequency ω_1 provided that the beam current exceeds the starting value. Electronic tuning may be accomplished by changing the sole voltage V_{So} or the cathode voltage V_{Co}, so as to vary the electron drift velocity. Amplitude modulation may be obtained by varying the accelerator voltage V_{Ao}, which varies the beam current.

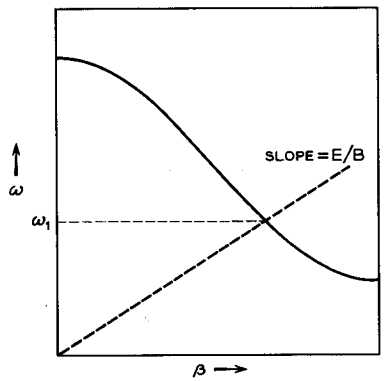

FIG. 12.3-2 Interaction using the backward-wave space harmonic. ω_1 is the radian frequency of oscillation.

Because of the phase focusing inherent in crossed-field devices, the exact frequency of oscillation is determined almost entirely by the circuit characteristics. That is, the frequency pushing (due to increasing the beam current) is very small.

Since the M-carcinotron is a crossed-field device, high-efficiency operation is possible. Efficiencies of 20 to 30 per cent are easily obtained.

The electron flow indicated in Figure 12.3-1 is perturbed by the rf electric field of the circuit. The perturbed electrons are shown in Figure 12.3-3 at a particular instant of time for a thin beam. Each electron moves in synchronism with the wave with a trajectory of the type previously discussed in connection with Figure 12-3.

For the purpose of discussion, half-cycle groups of electrons are identified by the letters A through G. Electrons A near the beginning of the circuit

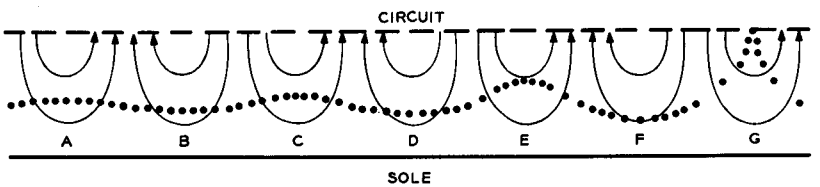

FIG. 12.3-3 Thin beam electrons and electric field lines at a particular instant of time in an M-carcinotron.

are moving toward the circuit, whereas electrons B are moving toward the sole. Farther down the circuit, electrons C are closer to the circuit, and electrons D are closer to the sole. However, electrons C have departed a greater distance from the unperturbed path than have electrons D. Thus, the electrons have lost a net amount of potential energy, this energy having been transferred to the rf field. The reason for the greater displacement of the electrons moving toward the circuit is that these electrons are in stronger rf fields, since they are closer to the circuit. Electrons E and F further illustrate this behavior. Electrons G have moved so far from the unperturbed position that some of them are being intercepted on the circuit.

In addition to the transverse motion of the electrons, there is also a bunching of the electrons in the longitudinal direction. Both of these effects cause induced currents in the circuit, and hence both effects must be considered in an analysis of the interaction process. Except for this added complexity, the analysis proceeds as for the backward-wave oscillator in Chapter 11. We shall not go into the details of this analysis. The interested reader is referred to the references.[20] The small-signal theory predicts the

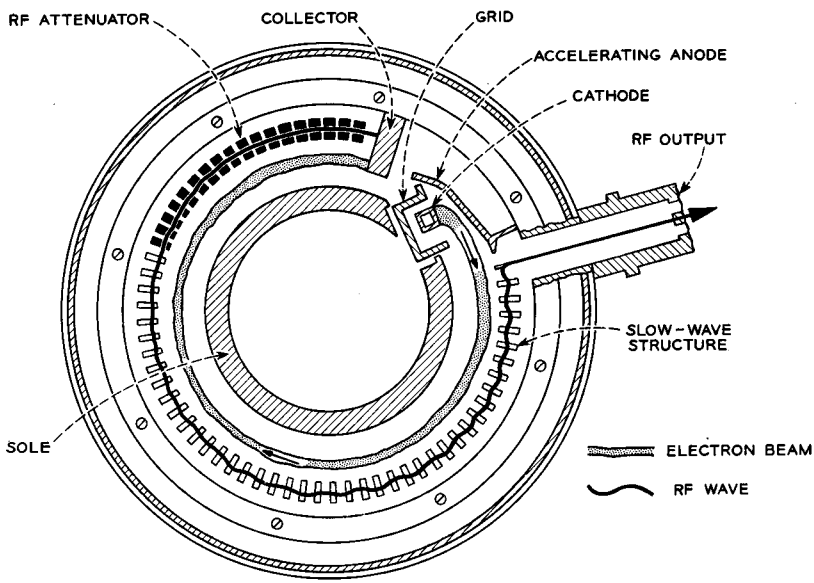

FIG. 12.3-4 Typical physical configuration of an M-carcinotron. The circular form of the device results in a lower magnet weight than would be required for a linear version. The rf attenuator shown serves to provide an rf termination for one end of the slow-wave structure. (Courtesy of Raytheon Company)

[20]Reference 12a, Vol. 1, pp. 395–495, 528–553, Reference 12.5.

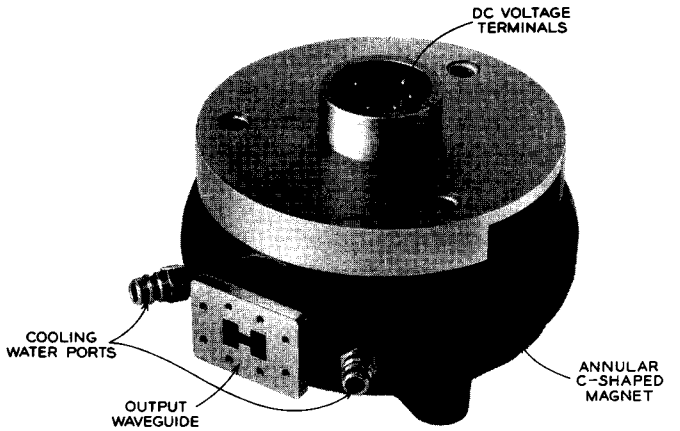

FIG. 12.3-5 Litton Industries L-3726 M-carcinotron. The tube weighs 16.5 pounds, with magnet. It measures approximately 18 cm in diameter and 13 cm high. (Courtesy of Litton Industries, Electron Tube Division)

starting current, and various large-signal, nonlinear theories allow one to estimate the efficiency. M-Carcinotrons are generally constructed in the circular re-entrant form shown in Figure 12.3-4. The slow-wave structure and sole are circular and nearly re-entrant to conserve magnet weight; the sole has the appearance of the cathode in a magnetron.

A typical M-carcinotron is the Litton L-3726, shown in Figure 12.3-5. The construction is similar to that of Figure 12.3-4. The circuit is an interdigital line,[21] a two-wire line with "fingers" extending alternately from one line toward the other. The tube delivers a minimum of 165 watts CW, voltage tunable over the frequency range 4800 to 6550 Mc.

TABLE 12.3-1. L-3726 TYPICAL OPERATING CHARACTERISTICS*

Frequency, Mc	4800 to 6550
Power output, watts	167 to 305
Cathode voltage, V_{Co}, volts	2045 to 4755
Accelerator voltage, V_{Ao}, volts	1615
Sole voltage, V_{So}, volts	2450
Cathode current, ma	300
Spurious output ratio, db (minimum)	15

*The symbols are defined in Figure 12.3-1.

Typical operating characteristics are summarized in Table 12.3-1. Tuning curves are shown in Figure 12.3-6. For this type of operation, tuning is

[21]See Problem 8.10.

accomplished by varying the cathode voltage V_{Co}. A faster rate of tuning is accomplished by varying the sole voltage, since the sole draws very little current and has only 65 picofarads of capacity to ground. However, with sole tuning the tuning range is limited to about 900 Mc with the other voltages held constant.

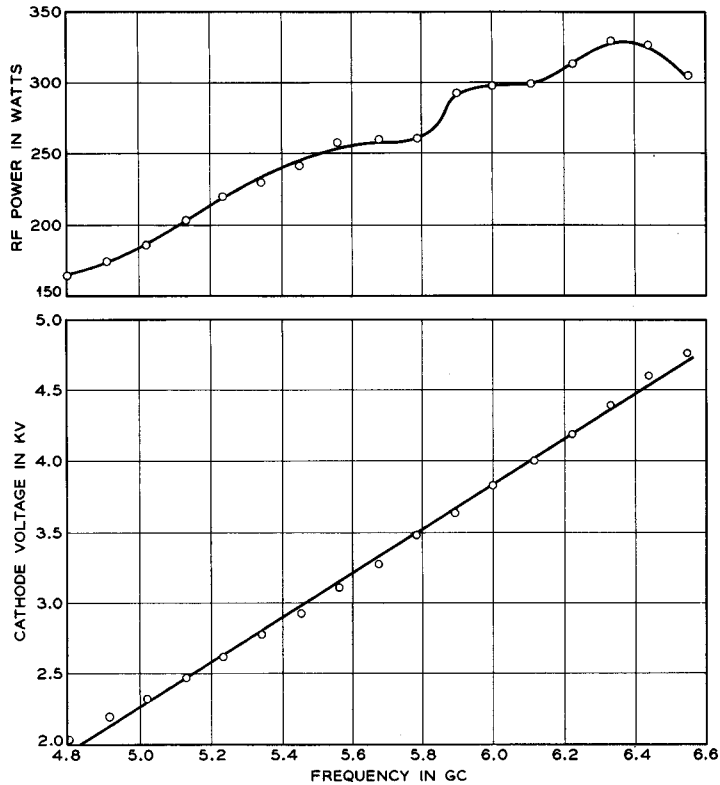

FIG. 12.3-6 Tuning curves for the L-3726. These data correspond to fixed values of sole voltage V_{So} and cathode current of 2450 volts and 300 ma, respectively. (Courtesy of Litton Industries, Electron Tube Division)

Examination of Figure 12.3-6 reveals that the frequency tuning with voltage is nearly linear. This feature allows a simplification of the circuitry associated with electronic tuning. Linear tuning results chiefly from the fact that the electron drift velocity is linearly related to the dc electric field in the interaction space, which in turn is directly proportional to the cathode voltage V_{Co}. In contrast, the electron velocity in the O-type back-

ward-wave oscillator is proportional to the square root of the tuning voltage. As a result, the tuning sensitivity of the M-type oscillator is higher.

The electronic efficiency of the L-3726 varies from 27.5 per cent at the low-frequency end to 24 per cent at the high end for the operating conditions given above.

A disadvantage of the M-carcinotron is a relatively high degree of spurious output, due to the inherent instability of electrons in crossed fields. The spurious output of the L-3726 is as much as 15 db below the desired signal. Because of this high noise level, M-carcinotrons have found considerable applications as high efficiency jamming sources for electronic countermeasures.

We may summarize our discussion of the M-carcinotron by comparing its characteristics with those of the O-type backward-wave oscillator. Both tubes are electronically tunable over large bandwidths. The M-carcinotron has the advantages of high efficiency, linear tuning, and low-frequency pushing. On the other hand, the M-carcinotron has considerably more noise or spurious output.

PROBLEMS

12.1 Derive Equation (12.1-19). Show that the velocity at the hub surface varies from ω/β at the Hartree voltage to $(eB/m)d$ at the Hull cutoff voltage.

12.2 Calculate the convection current density at the hub surface using the model of Figure 12.1-4 for a magnetron with the following parameters.

$$B = 7400 \text{ gauss}$$
$$V_{ao} = 17.5 \text{ kv}$$
$$d = 0.90 \text{ mm}$$

Ans.: 2560 amps/cm^2.

12.3 The electromagnetic fields in a magnetron operating in the π mode may be considered to be either those corresponding to a standing wave or the result of the superposition of two equal traveling waves carrying equal amounts of power but

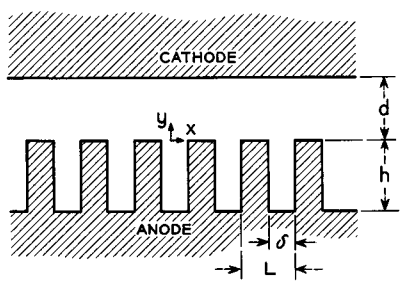

Problem 12.3

in opposite directions. The figure shows a linear version of a magnetron electrode configuration; this slow-wave structure is similar to that of Figure 8.7-4 and has similar properties.

(a) Sketch a Brillouin diagram for the lowest frequency mode of this structure over the range $-2\pi \leq \beta L \leq 2\pi$. Label the space harmonics. Indicate the point of interaction for the π-mode and indicate which two space harmonics are synchronous with the electrons at this point. Indicate which of the remaining space harmonics correspond to power flow in the same direction as each of the synchronous space harmonics.

(b) The x component of the rf electric field in the region between the vane tips and the cathode for power flow in the positive x direction is given by

$$E_{x+} = \frac{V_+}{L} \sum_{-\infty}^{\infty} \frac{\sinh \gamma_n(d-y)}{\sinh \gamma_n d} \frac{\sin \beta_n \delta/2}{\beta_n \delta/2} \epsilon^{-j\beta_n x}$$

where $\beta_n = \beta_o + (2\pi n/L)$ and $\gamma_n = \sqrt{\beta_n^2 - k^2}$, using an analysis similar to that given in Section 8.7(b). V_+ is the voltage across the vane-tip gap centered at $x = 0$. Write the corresponding expression for a wave having equal power flow in the negative x direction, if V_- instead of V_+ is the voltage across the gap centered at $x = 0$ in this case.

(c) For equal power flows in the two opposite directions $|V_+| = |V_-|$. Using this fact show that the four space harmonics discussed in part (a) have equal amplitudes at the frequency corresponding to π-mode operation.

(d) Show that the superposition of E_{x+} and E_{x-} corresponds to a standing wave, for π-mode operation.

12.4 Calculate the parameters of the equivalent circuit of Figure 12.1-19 as they apply to the Western Electric 7208B magnetron from the data given at the end of Section 12.1(c). Assume that Y_e is purely conductive.

12.5 A crossed-field amplifier is being operated under conditions corresponding to maximum gain at a given anode voltage. Is it possible to increase the gain of the device by increasing the circuit length, assuming that the anode voltage and other circuit parameters are held constant? Is it possible to increase the rf power output for the same rf power input by this means? Is it possible to decrease the rf power input for the same rf power output by this means? Explain.

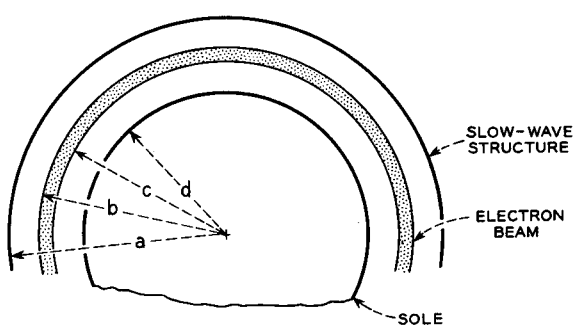

Problem 12.6

12.6 The figure shows ideal laminar flow in an M-carcinotron under dc conditions; that is, neglecting the effects of the rf fields. All electrons are assumed to follow circular paths, and the angular velocity is the same for all electrons independent of the radius. The latter condition allows exact synchronism of all electrons with the rf field despite the space-charge forces. Assuming that the electron charge density is uniform, independent of the radius, show that this ideal flow requires

$$V_{So} = \frac{\rho c^2}{4\varepsilon_o}\left(1 - 2 \ln \frac{c}{d}\right)$$

and

$$V_{Co} = -\frac{\rho b^2}{4\varepsilon_o}\left(1 + 2 \ln \frac{a}{b}\right)$$

where ρ is the electron charge density and the voltages are defined in Figure 12.3-1.

12.7 The Hull cutoff parabola and Hartree line as plotted in Figure 12.1-7 have been derived from a linear model of the magnetron. Show that curves of identical shape are obtained for the usual cylindrical model of the magnetron.

REFERENCES

A general reference on crossed-field devices is:

12a. E. Okress, Ed., *Crossed-Field Microwave Devices*, Academic Press, Inc., New York, 1961.

Two general references on magnetrons are:

12b. G. B. Collins, Ed., *Microwave Magnetrons*, McGraw-Hill Book Co., Inc., New York, 1948.

12c. J. C. Slater, *Microwave Electronics*, Chapter 13, D. Van Nostrand Co., Inc., Princeton, N. J., 1950.

Other references covering specific items are:

12.1 W. A. Smith, "A Wave Treatment of the Continuous Cathode Crossed-Field Amplifier," *Trans. IRE* **ED–9**, 379–387, September, 1962.

12.2 H. M. Olson and L. H. Von Ohlsen, "The Coaxial Magnetron, A Superior Microwave Power Source," *IRE Wescon Convention Record*, Vol. 2, Part 1, August, 1961.

12.3 W. C. Brown, "Description and Operating Characteristics of the Platinotron—A New Microwave Tube Device," *Proc. IRE* **45**, 1209–1222, September, 1957.

12.4 W. A. Smith and F. Zawada, "A 3-Megawatt, 15-Kilowatt S-Band Amplitron," *Microwave Journal* **2**, 42–45, October, 1959.

12.5 A. H. W. Beck, *Space-Charge Waves and Slow Electromagnetic Waves*, Pergamon Press, Inc., New York, pp. 256–270, 1958.

12.6 N. R. Mantena and T. Van Duzer. "Low Noise and Space-Charge Smoothing in a Crossed-Field Amplifier," *Proc. IEEE* **51**, 1662, 1663, November, 1963.